Biosafety and Health 6 (2024) 350–360

Contents lists available at ScienceDirect

Biosafety and Health

journal homepage: www.elsevier.com/locate/bsheal

Original Research

Rapid generation and characterization of recombinant HCoV-OC43-VR1558 infectious clones expressing reporter Renilla luciferase

Fei Ye [a,1], Na Wang [a,b,1], Qiongge Guan [a,b,1], Mengwei Wang [a,b], Jiewei Sun [a,b], Desheng Zhai [c], Baoying Huang [a,*], Ying Zhao [b,*], Wenjie Tan [a,2,*]

[a] National Key Laboratory of Intelligent Tracking and Forecasting for Infectious Diseases, NHC Key Laboratory of Biosafety, National Institute for Viral Disease Control and Prevention, Chinese Center for Disease Control and Prevention, Beijing 102206, China
[b] School of Pharmacy, Xinxiang Medical University, Xinxiang 453003, China
[c] School of Public Health, Xinxiang Medical University, Xinxiang 453003, China

ARTICLE INFO

Article history:
Received 16 August 2024
Revised 17 November 2024
Accepted 17 November 2024
Available online 19 November 2024

Keywords:
Infectious clones
Human coronaviruses (HCoV)-OC43
Transformation-associated recombination (TAR)
Reporter Renilla luciferase (Rluc)

ABSTRACT

Viral infectious clones (ICs) serve as robust platforms for studying viral biology and screening antiviral agents using reverse genetics. However, the molecular profiles and complex limitations of human coronaviruses (HCoVs) pose a challenge to ICs development. In this study, we report a novel platform to develop the ICs for HCoV-OC43-VR1558 using a one-step assembly method in yeast by transformation-associated recombination (TAR) technology. Recombinant HCoV-OC43-VR1558, named as rOC43(1558)-WT, was rapidly generated by TAR. In addition, recombinant HCoV-OC43-VR1558-expressing reporter genes, named as rOC43(1558)-ns2FusionRluc, was also generated based on TAR by inserting the ns2 region of the IC with Renilla luciferase (Rluc). We further characterized their replication through virus titration using 50 % tissue culture infective dose ($TCID_{50}$) and indirect immunofluorescence assay (IFA), luciferase reporter assay, and western blotting (WB) assay. The genetic stability of the recombinant HCoV-OC43 was assessed through viral genome sequencing following passaging in BHK-21 cells. These reporter viruses were validated as screening tools for inhibitors *in vitro* by evaluating the antiviral activities of remdesivir and chloroquine. The phenotypes of HCoV-OC43-VR1558 and HCoV-OC43-VR759 were compared *in vitro* and *in vivo*. The TAR-based one-step assembly of IC was successfully applied, facilitating the rapid generation of recombinant HCoV-OC43 and providing a useful platform for the investigation of biological mechanisms, development of vaccines and diagnostic tests, and screening inhibitors of HCoVs.

1. Introduction

Coronaviruses (CoVs) are enveloped viruses with positive-sense single-stranded ribonucleic acid (RNA) genomes of approximately 30 kb. They are widespread in animals and can cause a range of respiratory or enteric diseases in humans, varying from mild-to-severe [1,2]. Seven human CoVs (HCoV) have been identified, including HCoV-229E, HCoV-OC43, HCoV-NL63, HCoV-HKU1, severe acute respiratory syndrome (SARS)-CoV, Middle East respiratory syndrome (MERS)-CoV and SARS-CoV-2. The global pandemic coronavirus disease 2019 (COVID-19) was caused by the SARS-CoV-2. As of October 6, 2024, more than 776 million cases of COVID-19 and over 7.0 million fatalities have been reported globally (https://covid19.who.int/). To prepare for the future pandemics caused by HCoVs, a comprehensive understanding of the HCoVs biology and the development of preventive and therapeutic measures against HCoVs are essential.

Generating recombinant viruses using reverse genetics approaches represents a powerful tool for addressing important questions regarding the biology of viral infections, including the mechanisms, pathogenesis, and diseases [3]. The use of reverse genetics techniques also offers the possibility of generating recombinant viruses expressing reporter genes for use in cultured cells or *in vivo* models of infection, whereby reporter gene expression can be used as a valid surrogate to identify the presence of the virus in infected cells [4,5]. Several HCoVs infectious clones (ICs) have been constructed, although this

* Corresponding authors: National Key Laboratory of Intelligent Tracking and Forecasting for Infectious Diseases, NHC Key Laboratory of Biosafety, National Institute for Viral Disease Control and Prevention, 155 Changbai Road, Changping District, Beijing 102206, China (W. Tan and B. Huang); School of Pharmacy, Xinxiang Medical University, Xinxiang 453003, China (Y. Zhao).

E-mail addresses: huangby@ivdc.chinacdc.cn (B. Huang), zhaoyingxxmc@163.com (Y. Zhao), tanwj@ivdc.chinacdc.cn (W. Tan).

[1] These authors contributed equally to this work.

[2] Given his role as Editorial Board Member, Wenjie Tan had no involvement in the peer-review of this article and had no access to information regarding its peer review. Full responsibility for the editorial process of this article was delegated to Guest Editor Qiang Ding.

https://doi.org/10.1016/j.bsheal.2024.11.006

HIGHLIGHTS

Scientific question

Genome-wide reassembly of coronavirus infectious clones has long been hampered by the large size of the viral genome (–30 kb) and the presence of several toxic viral sequences that limit standard molecular cloning strategies.

Evidence before this study

Rapid construction of recombinant virus-carrying reporter genes by reverse genetics provided an important strategy for the high-throughput, visualization, and safe operation of coronaviruses. The development of infectious clones for human coronaviruses (HCoVs)-OC43 VR1558 and VR759 with methods of *in vitro* transcription and bacterial artificial chromosome have been reported. However the comparison studies for HCoV-OC43 VR759 and VR1558 were limited.

New findings

HCoV-OC43 VR1558 wild type [rOC43(1558)-WT] and reporter virus expressing Renilla luciferase [rOC43(1558)-ns2FusionRluc] were constructed by transformation-associated recombination technology in yeast. A high-throughput and visualization anti-coronavirus inhibitor platform was established with the reporter virus *in vitro* and *in vivo*. A comparison study for HCoV-OC43 VR759 and VR1558 demonstrated that, although more significant cytopathic effects for VR1558 *in vitro,* HCoV-OC43 VR759 exhibited higher virulence than that of the VR1558 in mice model.

Significance of the study

The luciferase readout of the reporter virus rOC43(1558)-ns2FusionRluc can be used to visually reflect the neurological symptoms caused by coronavirus infection and to evaluate broad-spectrum anti-coronavirus inhibitors *in vitro* and *in vivo*.

has proven difficult, given the length of the viral genome and the presence of unstable viral complementary deoxyribonucleic acid (cDNA) regions in bacteria [6,7]. During the past two decades, with the advancement in modern molecular tools and reagents, several creative approaches, including the vaccinia virus vector method [4,8,9], *in vitro* ligation [10,11], bacterial artificial chromosome (BAC) [12,13], yeast artificial chromosome (YAC) [14–16], cyclic polymerase extension reaction (CPER) [17,18] and the recently reported infectious subgenome amplicon (ISA) technology [19]. Consequently, there is a need to explore alternative strategies to overcome these limitations.

HCoV-OC43, an endemic low-risk HCoVs belonging to the betacoronavirus family, was first isolated from a patient with upper respiratory tract disease in the 1960s. It has garnered attention as an attractive and safe model for studying HCoVs in the low-risk research setting [biosafety level (BSL)-2]. In contrast, highly pathogenic betacoronaviruses, such as SARS-CoV, MERS-CoV, and SARS-CoV-2, require the use of a cumbersome BSL-3 confinement facility. Patients infected with MERS-CoV and SARS-CoV-2 have displayed some neurological symptoms [20,21], while patients infected with HCoV-OC43 also had reported to suffer from fatal encephalitis [22]. Previous research had utilized HCoV-OC43 as a safe surrogate for studying SARS-CoV-2 [23].

Several approaches have been reported to assemble HCoV-OC43 infectious clones, contributing significantly to the screening of antivirals against coronavirus. Currently, the most widely used HCoV-OC43 strains include the VR759 and VR1558 (American Type Culture Collection, ATCC). The HCoV-OC43 VR1558 is a tissue culture adapted variant of VR759, which was originally derived from a virus passaged in mice (https://www.atcc.org/products/vr-1558). BAC platform for the HCoV-OC43-VR759 strain IC has been reported [13]. Subsequently, several ICs of HCoV-OC43-VR759 were generated and used for functional characterization and high-throughput screening assays [24–31]. To date, the development of a recombinant HCoV-OC43 VR1558 reporter virus expresses nano-luciferase by the method of *in vitro* transcription has been demonstrated and applied for screening antiviral compounds against coronaviruses [32]. However, no comparison studies of HCoV-OC43 VR759 and VR1558 were reported.

The transformation-associated recombination (TAR) technology is a one-step assembly method that utilizes a highly efficient homologous recombination system in yeast to assemble multiple DNA fragments with overlapping sequences [33]. This method employs the pYES1L vector, a linearized BAC / YAC shuttle vector capacity of cloning up to 110 kb of DNA fragments [34]. Due to its ability to facilitate homologous recombination in yeast and the high stability of the construct in *Escherichia coli* (*E. coli*), the TAR cloning technology has been successfully applied to assemble the full-length cDNA clone of several coronaviruses [14–16].

In this study, a novel infectious cDNA clone of HCoV-OC43-VR1558 was rapidly generated through one-step assembly in yeast using the TAR technology with the pYES1L vector. The recombinant HCoV-OC43 (rHCoV-OC43) was successfully rescued, and its replication, reporter expression, and genetic stability were investigated. The reporter virus was effectively employed to evaluate the antiviral activities of remdesivir and chloroquine *in vitro* and *in vivo*. Furthermore, this study compared the phenotypes of rHCoV-OC43-VR1558 and rHCoV-OC43-VR759 both *in vitro* and *in vivo*.

2. Materials and methods

2.1. Cell, virus, plasmids, and antibodies

BHK-21 (ATCC no. CCL-10) and HEK-293T (ATCC no. CRL-3216) cells were cultured in Dulbecco's Modified Eagle's Medium (DMEM) supplemented with 10 % fetal bovine serum (FBS). HCoV-OC43 was obtained from ATCC (VR-1558). Viruses of rOC43(759)-WT and rOC43(759)-ns2DelRluc used in this study were previously rescued in our laboratory [29]. The HCoV-OC43 nucleocapsid antibody (40643-T62) was purchased from Sino Biological (Beijing, China) and anti-β-actin (13E5) rabbit monoclonal antibodies were obtained from Cell Signaling Technology (Danvers, MA, USA).

2.2. Construction and rescue of rOC43(1558)-WT and rOC43(1558)-ns2FusionRluc

The full-length cDNA clone of HCoV-OC43 was constructed using the TAR technology, with the pYES1L vector (Thermo Fisher, USA) containing the YAC / BAC, as previous reports [34]. The YAC / BAC enables this infectious cDNA clone replicate in both yeast and *E. coli.* Recombinant viruses were rescued from the infectious cDNA clones pYB-rOC43(1558)-WT and pYB-rOC43(1558)-ns2FusionRluc. Briefly, eight overlapping DNA fragments were amplified and assembled into pYB-rOC43(1558)-WT. To facilitate the assembly of the viral genome and incorporate genetic tags to distinguish the rOC43(1558)-WT clone from the natural isolate, a silent mutation was introduced in the viral *N* gene [29,309 nucleotides (nt) G → A]. To generate the reporter-expressing rOC43(1558)-ns2FusionRluc, the non-structure (ns) 2 gene was modified with Rluc in the pYB-rOC43(1558)-WT plasmid carrying the remaining viral genome, to produce pYB-rOC43(1558)-

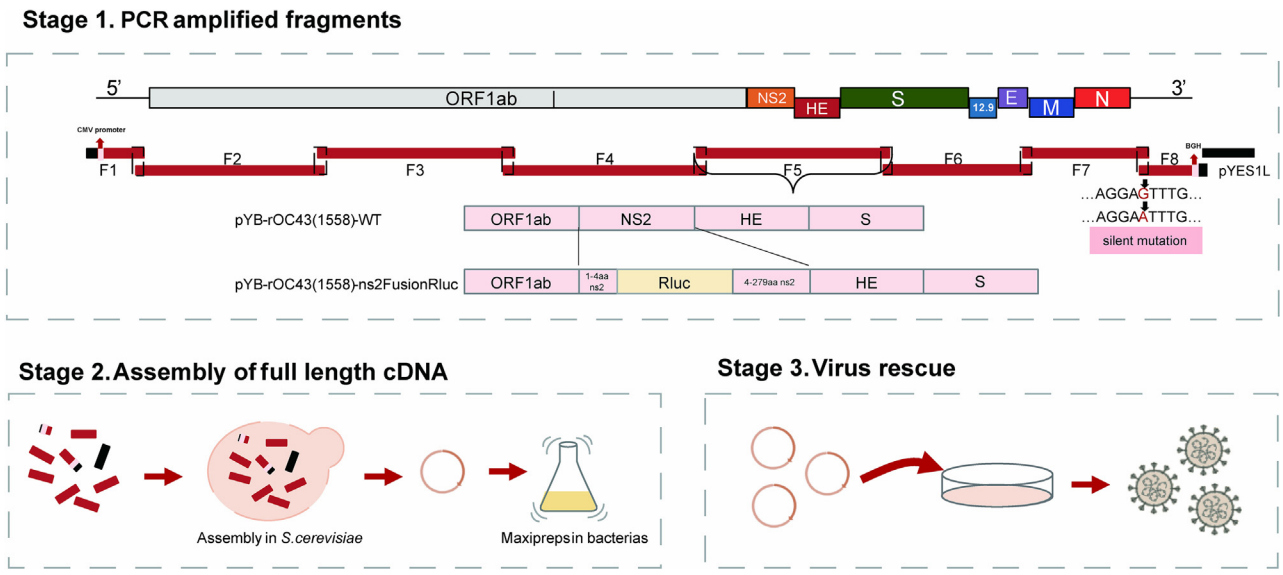

Fig. 1. Assembly of HCoVs-OC43 infectious clones. Strategy for TAR of HCoV-OC43 full-length cDNA clone fragments in yeast. The genome structure of HCoV-OC43 relevant sequences is indicated. Abbreviations: HCoVs, human coronaviruses; cDNA, complementary deoxyribonucleic acid; TAR, transformation-associated recombination; PCR, polymerase chain reaction; CMV, cytomegalovirus promoter; ORF, open reading frame; BGH, bovine growth hormone termination.

ns2FusionRluc plasmids for viral rescue (Fig. 1). The construct strategy was followed previous reports [29,34].

The successful recovery of rOC43(1558)-WT was confirmed by indirect immunofluorescence assay (IFA) and western blot (WB) analysis. In this study, no helper plasmid expressing the nucleoprotein (NP) gene was utilized. Therefore, the expression of NP for the rescued virus rOC43(1558)-WT and rOC43(1558)-ns2FusionRluc infected BHK-21 cells at a multiplicity of infection (MOI) of 0.01 was determined with anti-OC43-NP-PcAb. As the molecular weight for NP and β-actin are very closely, the WB analysis was conducted in two different gels. More details are described in the Supplemental Materials.

2.3. Reporter-based inhibition assay for identifying anti-HCoVs

BHK-21 cells were inoculated in a 96-well plate with rescued viruses at a MOI of 0.01 for 1 h at 33 °C. Following viral adsorption, cells were washed and incubated in 100 μL of infection medium (DMEM with 2 % FBS) containing three-fold serial dilutions of remdesivir, chloroquine or 0.1 % dimethyl sulfoxide (DMSO) as vehicle control. After 72 h, the cells in each well were assayed for relative light units (RLU) using the Renilla-Glo luciferase assay system (Promega) following the manufacturer's protocol.

2.4. Animal experiments

10-day-old BALB / c suckling mice were obtained from Sibeifu Beijing Biotechnology (Beijing, China). BALB / c mice were intracerebrally inoculated with rOC43(759)-ns2DelRluc, rOC43(1558)-ns2FusionRluc, or rOC43(1558)-WT for subsequent assays. For comparative analysis, the BALB / c suckling mice were randomly divided into groups, with one group mice were intracranially inoculated with 2×10^2 50 % tissue culture infective dose ($TCID_{50}$) rOC43(759)-ns2DelRluc as control. The remaining groups were intracranially incubated with 2×10^6 $TCID_{50}$, 2×10^4 $TCID_{50}$, and 2×10^2 $TCID_{50}$ of the recombinant virus rOC43(759)-ns2DelRluc or rOC43(1558)-ns2FusionRluc according to previous trials in our laboratory and the references [27,35–38]. The experiment followed previous reports [27]. Additional details are provided in the Supplementary Materials.

2.5. Protein structural modelling

The structure of the HCoV-OC43 S glycoprotein trimer was predicted using the web-based homology modelling server, SWISS-MODEL (https://swissmodel.expasy.org/). A Basic Local Alignment Search Tool for protein (BLASTp) search was performed against the Protein Data Bank (PDB) (https://www.rcsb.org/pdb) using default parameters to identify suitable templates for homology modelling. Based on its high sequence identity, QMEAN Z-score, coverage, and low e-value, the crystal structure of HCoV-OC43 S (PDB code: 6owb) was selected as the template.

2.6. Statistical analysis

Statistical analyses were performed using GraphPad Prism 8. Differences were considered statistically significant using Student's *t* test. Differences were considered statistically significant at $P < 0.05$.

3. Results

3.1. Characterization of rOC43(1558)-WT and rOC43(1558)-ns2FusionRluc in vitro

The full-length cDNA clone of pYB-rOC43(1558)-WT was successfully constructed and confirmed by sequencing. The designed silent mutation for the *N* gene (G29309A) of rOC43(1558)-WT was verified by DNA sequencing analyses (Fig. 2A).

Subsequently, N protein expression levels were evaluated by western blotting using cell lysates from either rOC43(1558)-WT or rOC43(1558)-ns2FusionRluc-infected cells and using antibodies against the viral NP and β-actin as a loading control (Fig. 2B). As expected, viral NP expression was detected in the lysates of all viruses, indicating that the recombinant virus could be stably passaged *in vitro*. As the Rluc reporter was inserted into NS2 region and does not affect the molecular weight of N protein, there is no difference in the size of the NP pro-

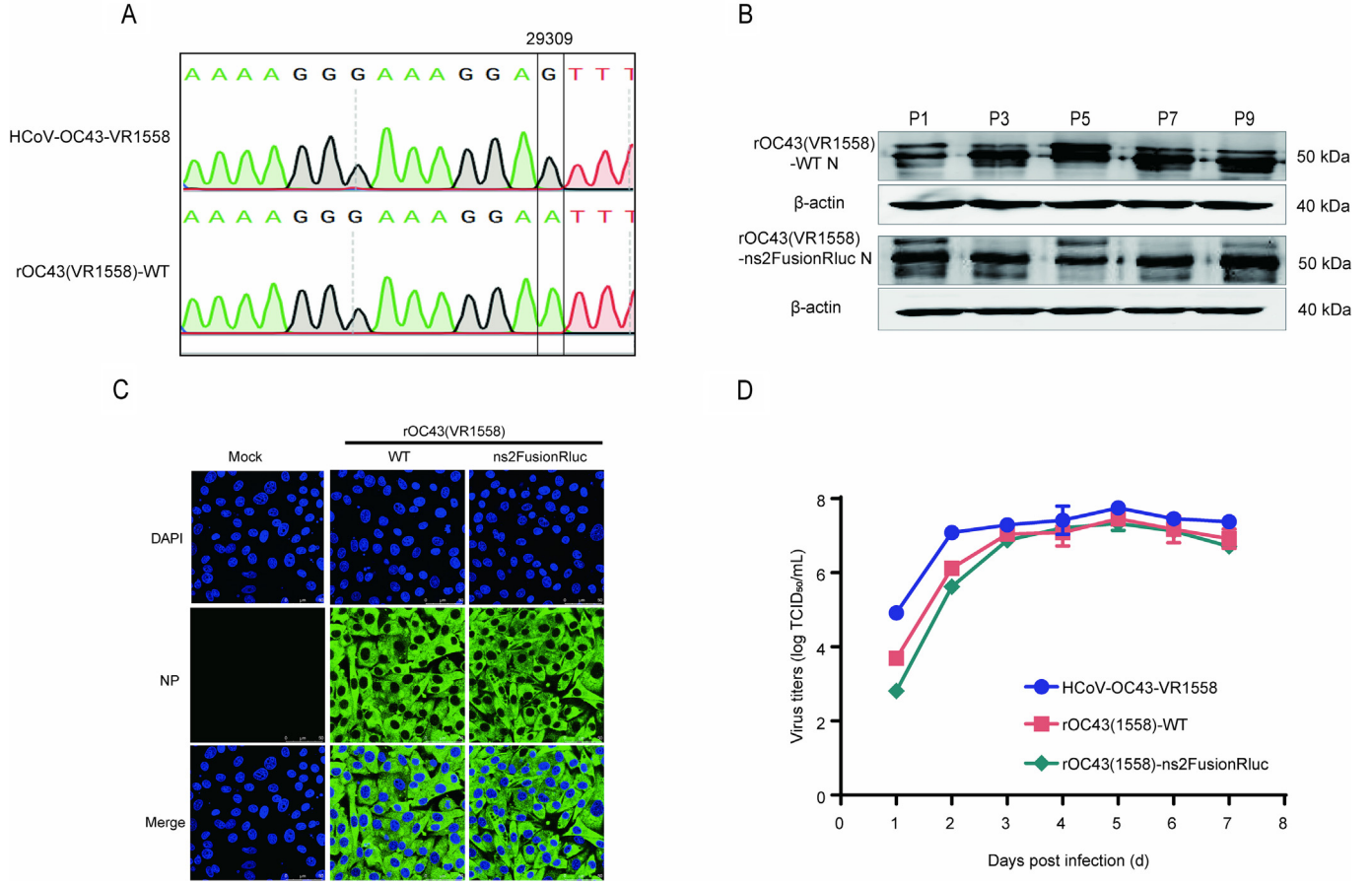

Fig. 2. Characterization of recombinant HCoVs-OC43 (rHCoV-OC43). A) Chromatograms of Sanger sequencing results. Silent mutation introduced to the site (G to A) is shown in the black box. B) Western blot analysis of N protein expression of rOC43(1558)-WT and rOC43(1558)-ns2FusionRluc. BHK-21 cells were infected (MOI of 0.01) with various passages of rOC43(1558)-WT or rOC43(1558)-ns2FusionRluc, and lysed for western blotting to monitor the expression of N protein. β-actin was used as a loading control. C) Fluorescence analysis of HCoV-OC43 infected cells. BHK-21 cells were infected with rOC43(1558)-WT or rOC43(1558)-ns2FusionRluc at an MOI of 0.01. Cells were fixed and immune-stained with a polyclonal antibody against the HCoV-OC43 N protein 24 hpi. Goat anti-rabbit IgG H&L (Alexa Fluor® 488, green) secondary antibodies were used, and nuclei were visualized with DAPI. Scale bars represent 50 μm. D) Replication kinetics of HCoV-OC43-VR1558, rOC43(1558)-WT, and rOC43(1558)-ns2FusionRluc. BHK-21 cells were infected (MOI of 0.01) with HCoV-OC43-VR1558, rOC43(1558)-WT, and rOC43(1558)-ns2FusionRluc. At 1, 2, 3, 4, 5, 6, and 7 days post-infection, the presence of infectious virus in the tissue culture supernatants was determined using a $TCID_{50}$ assay. Abbreviations: HCoVs, human coronaviruses; MOI, multiplicity of infection; $TCID_{50}$, 50 % tissue culture infective dose; hpi, hours post-infection; DAPI, 4′,6-diamidino-2-phenylindole; NP, nucleoprotein; WT, wild type.

tein between rOC43(1558)-WT and rOC43(1558)-ns2FusionRluc as confirmed by the marker labels. Similarly, the successful recovery of rHCoV-OC43 was confirmed by indirect immunofluorescence assay (IFA) using an antibody against HCoV-OC43 NP to detect rHCoV-OC43 infection (Fig. 2D).

To determine whether the recombinant viruses displayed similar growth kinetics as the parental strain, the growth kinetics were assessed at different times post infection. The BHK-21 cells were infected with HCoV-OC43-VR1558, rOC43(1558)-WT and rOC43 (1558)-ns2FusionRluc. Virus titers were determined and compared. As shown in Fig. 2C, all recombinant viruses exhibited similar growth kinetics. The titre for HCoV-OC43-VR1558 was slightly higher than that of the other viruses.

3.2. Reporter-based inhibition assay for the identification of antivirals in vitro and in vivo

To demonstrate the sensitivity of rHCoV-OC43 to coronavirus (CoVs) inhibitors with different mechanisms of action, several inhibition experiments were conducted in BHK-21 cells. The compounds selected for initial studies were remdesivir and chloroquine. Replication inhibition was determined by measuring the reduction of viral RNA copies numbers or luciferase activities relative to DMSO control-treated cells at 72 h post-infection (hpi). As shown in Fig. 3 A–D, both compounds exhibited antiviral activities in a dose-dependent manner, using either copies or luciferase as a readout. The half maximal effective concentration (EC_{50}) of chloroquine in inhibiting the rOC43(1558)-ns2FusionRluc replication, as determined either using percent viral copies or percent luciferase activity, were 0.66 or 0.50 μmol/L, respectively. For remdesivir, the EC_{50} for inhibiting rOC43(1558)-ns2FusionRluc replication, determined by either viral copies or luciferase activity, was 0.28 or 0.78 μmol/L, respectively. The EC_{50} values obtained from both methods were comparable, highlighting the advantage of luciferase-based readouts for fast assay development.

To assess the potential utility of bioluminescence imaging (BLI) in rOC43(1558)-ns2FusionRluc-infected mice for evaluating the efficacy of antiviral drugs *in vivo*, mice were administered chloroquine 2 h prior to viral inoculation on day 0 at a dose of 30 mg/kg, with subsequent daily administration, following a previous study on HCoV-OC43-WT [27]. Mice were intracerebrally infected with 2×10^6 $TCID_{50}$ of rOC43(1558)-ns2FusionRluc, and BLI was measured daily (Fig. 3E),

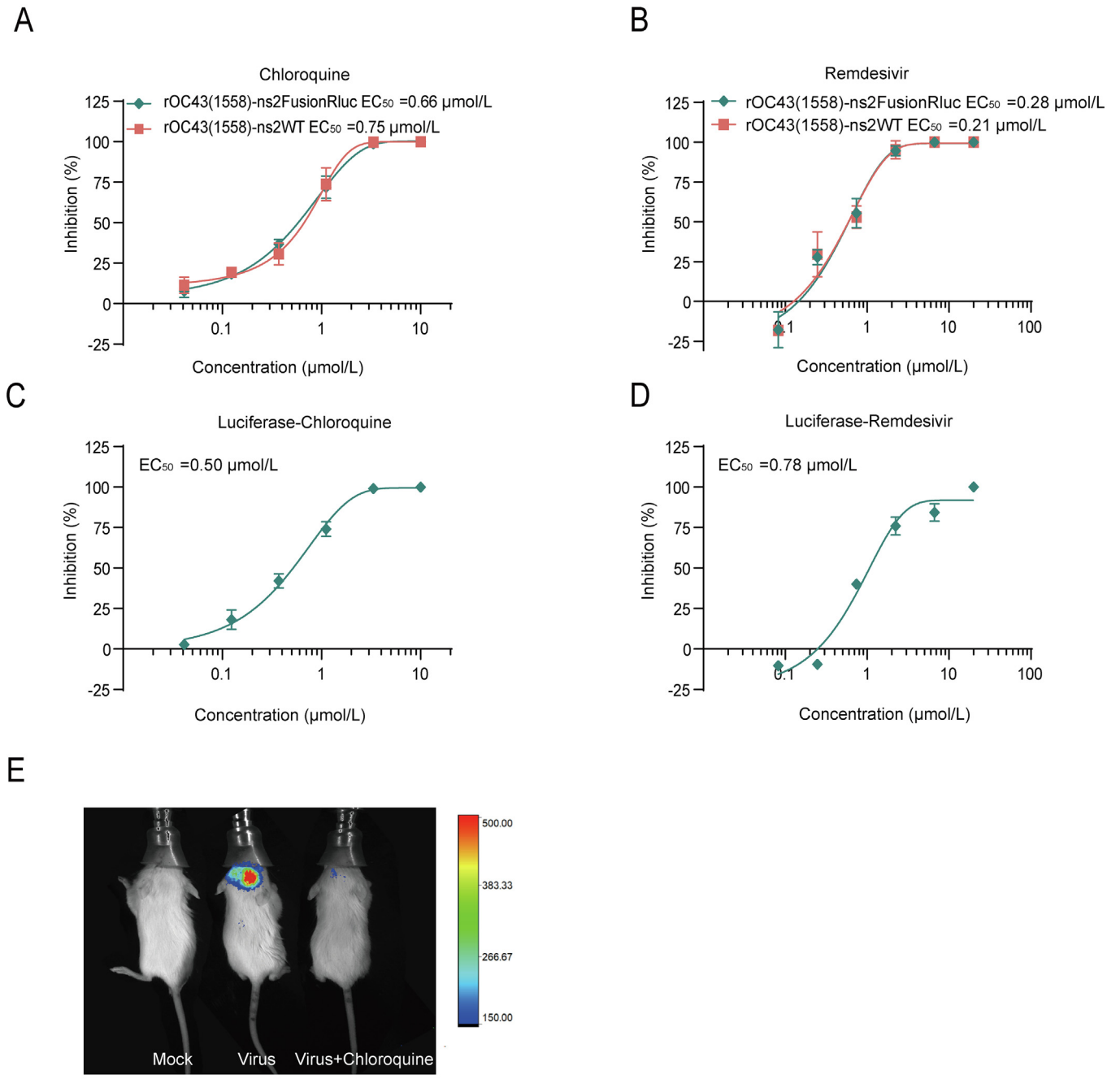

Fig. 3. Reporter-based inhibition assay for the identification of antivirals agents. The dose-dependent responses of HCoVs-OC43-VR1558 activity to chloroquine and remdesivir were assessed. BHK-21 cells were either mock-treated or infected with MOI of 0.01 with rOC43(1558). At 1 h post-infection, medium containing three-fold serial dilutions of chloroquine (A, C) and remdesivir (B, D) was added to the cells. At 72 h post-infection, EC_{50} was determined using a dose–response curve drawn based on viral RNA copies in infected cells using four-parameter nonlinear regression. In the case of cells infected with rOC43(1558)-ns2FusionRluc, luciferase activity was determined at 72 h post-infection by a luciferase assay. The activities were determined by luciferase signals compared to dimethyl sulfoxide-treated cells. E) BLI of BALB / c mice treated with or without chloroquine after rOC43(1558)-ns2FusionRluc inoculation. Mice infected intracerebrally with 10^6 of $TCID_{50}$ of rOC43(1558)-ns2FusionRluc were either untreated (intermediate panel) or treated (right panel) with chloroquine (30 mg/kg) daily, followed by daily measurement of BLI by intraperitoneal injection of Rluc substrate and capture of photon emission using the *in vivo* F Pro system. A representative BLI image from one mouse is shown. Abbreviations: HCoVs, human coronaviruses; MOI, multiplicity of infection; EC_{50}, the half maximal effective concentration; BLI, bioluminescence imaging; $TCID_{50}$, 50 % tissue culture infective dose; Rluc, Renilla luciferase.

confirming the disparity in rOC43(759)-ns2DelRluc replication between mice treated with or without chloroquine. These findings demonstrate the potential of rOC43-ns2DelRluc-infected mice as a highly responsive *in vivo* model for evaluating the efficacy of antiviral drugs targeting HCoV-OC43 and compounds with activities against a broad spectrum of CoVs.

3.3. Comparison of biological characteristics of HCoV-OC43

The differences between the HCoV-OC43-VR1558 and HCoV-OC43-VR759 were evaluated both *in vitro* and *in vivo*. We characterized HCoV-OC43-VR1558 and HCoV-OC43-VR759 by assessing the differential development of cytopathic effects (CPE) and the expres-

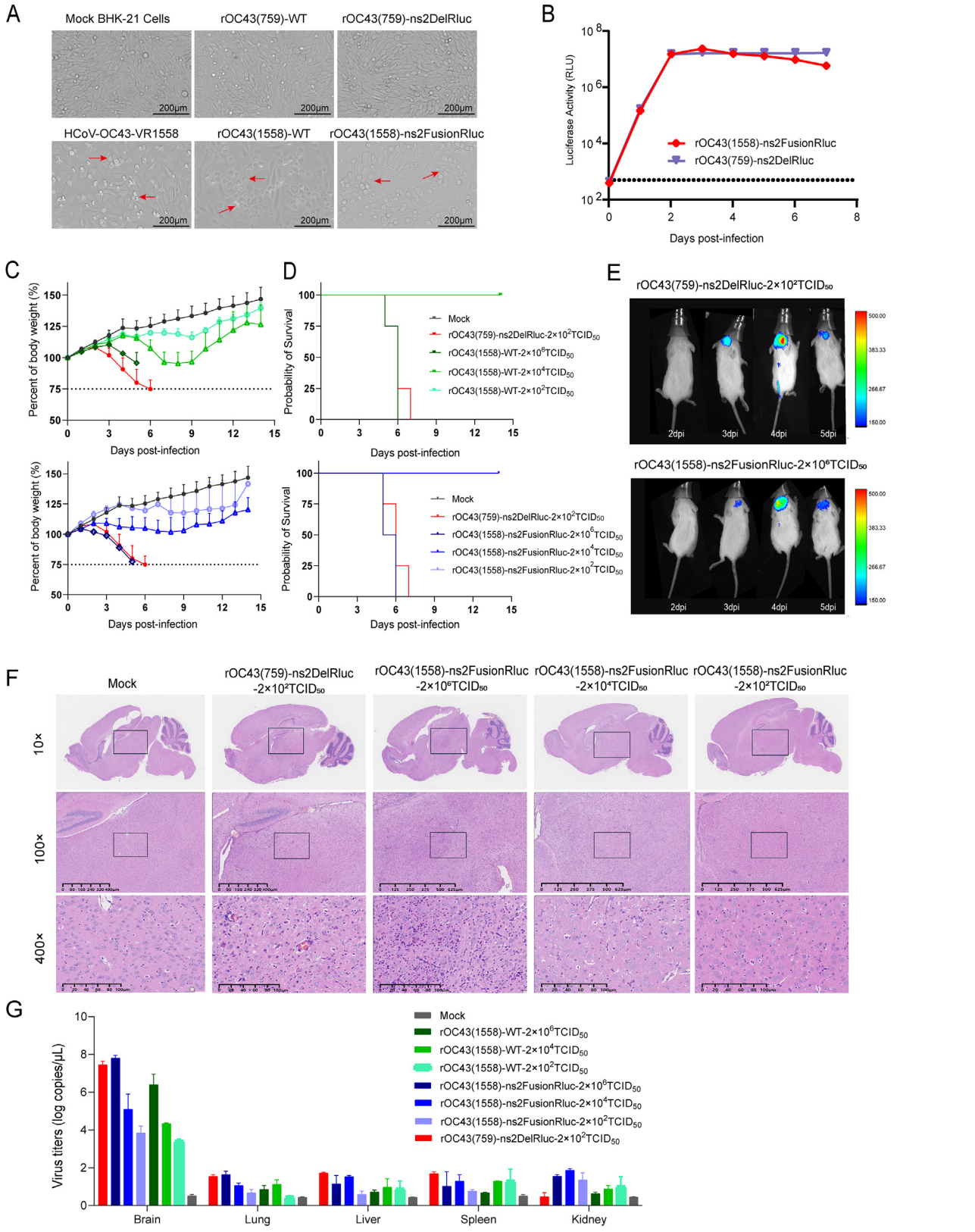
A
Mock BHK-21 Cells
rOC43(759)-WT
rOC43(759)-ns2DelRluc
HCoV-OC43-VR1558
rOC43(1558)-WT
rOC43(1558)-ns2FusionRluc
200μm
B
Luciferase Activity (RLU)
Days post-infection
rOC43(1558)-ns2FusionRluc
rOC43(759)-ns2DelRluc
C
Percent of body weight (%)
Days post-infection
D
Probability of Survival
Mock
rOC43(759)-ns2DelRluc-2×10²TCID50
rOC43(1558)-WT-2×10⁶TCID50
rOC43(1558)-WT-2×10⁴TCID50
rOC43(1558)-WT-2×10²TCID50
rOC43(1558)-ns2FusionRluc-2×10⁶TCID50
rOC43(1558)-ns2FusionRluc-2×10⁴TCID50
rOC43(1558)-ns2FusionRluc-2×10²TCID50
E
rOC43(759)-ns2DelRluc-2×10²TCID50
rOC43(1558)-ns2FusionRluc-2×10⁶TCID50
2dpi
3dpi
4dpi
5dpi
F
Mock
rOC43(759)-ns2DelRluc -2×10²TCID50
rOC43(1558)-ns2FusionRluc -2×10⁶TCID50
rOC43(1558)-ns2FusionRluc -2×10⁴TCID50
rOC43(1558)-ns2FusionRluc -2×10²TCID50
10×
100×
400×
G
Virus titers (log copies/μL)
Brain
Lung
Liver
Spleen
Kidney

sion levels of Rluc in cell cultures. Compared to rOC43(759)-WT, cells infected with HCoV-OC43-VR1558 exhibited typical CPE characterized by cell shedding, fusion, and a high refractive index (Fig. 4A). There was no significant increase in Rluc expression levels observed for rOC43(759)-ns2DelRluc and rOC43(1558)-ns2FusionRluc, but high levels of Rluc expression were detected in the culture supernatants of both rOC43(759)-ns2DelRluc- and rOC43(1558)-ns2FusionRluc-infected cells (Fig. 4B).

For comparative analysis, BALB / c mice were intracranially inoculated with rOC43(1558)-WT, rOC43(1558)-ns2FusionRluc, and rOC43(759)-ns2DelRluc. In the low-dose infection group of rOC43(759)-ns2DelRluc2 $\times$ 10^2 $TCID_{50}$, mice body weight decline started on day 3 post infection (DPI), accompanied by the development of a hunched back by day 4 DPI, followed by restlessness, leading to mortality by day 5, with complete fatality by day 7 DPI. Similar symptoms were observed in the rOC43(1558)-WT and rOC43(1558)-ns2FusionRluc infection groups, but only for high-dose of 2 $\times$ 10^6 $TCID_{50}$ (Fig. 4C and 4D).

In vivo imaging demonstrated Rluc signals in the brain tissues on the third-day post-infection, reaching peak signals on the fourth day for both strains. These findings indicated that both HCoV-OC43 strains primarily induced neurological symptoms in mice (Fig. 4E). However, the luciferase signals were observed only under high-dose conditions, 2 $\times$ 10^6 $TCID_{50}$. At a dose of 2 $\times$ 10^2 $TCID_{50}$, the rOC43(1558) strain exhibited lower virulence in mice compared to the rOC43(759) strain (data not shown). No significant pathological changes were observed in the cortex, hippocampus, thalamus, and other regions of the brain in the mock mice. However, neuronal condensation, necrosis, nuclear fragmentation, and disintegration can be observed in various regions of the mouse brain, particularly in the hippocampus in rOC43(759)-ns2DelRluc infected mice. In the rOC43 (1558)-ns2FusionRluc virus infection groups, with the increased virus dose, more severe symptoms appeared, such as neuronal condensation and necrosis, nuclear fragmentation and disintegration, residual and unquantifiable cell fragments, and infiltration of inflammatory cells such as microglia and lymphocytes (Fig. 4F). Following the infection with both viral strains, viral RNA was predominantly detected in the brain tissues (Fig. 4G). We successfully established a lethal mouse infection model using the rOC43(1558) strain, and an *in vivo* animal model employing the rOC43(1558)- ns2FusionRluc strain.

As the introduction about HCoV-OC43 VR-1558 on the website of ATCC, the HCoV-OC43 VR-1558 is a tissue culture-adapted item derived from virus passaged in mice (ATCC VR-759). The complete genome sequence for ATCC VR-1558 exhibits over 98 % homology to that of VR-759 (AY585228.1). To explore the molecular basis of phenotype between HCoV-OC43-VR1558 and HCoV-OC43-VR759, we investigate the divergence in the amino acids of rOC43(1558)-WT and rOC43(759)-WT strain. Compared to rOC43(759)-WT, the rOC43(1558)-WT strain harbours 38 amino acids differences, of which 21 are located in the spike protein's coding region, including 17 amino acid mutation and 4 amino acid insertion (see Table 1). The specific amino acid positions of HCoV-OC43 spike domain are illustrated in Fig. 5A, while Fig. 5B depicts the four insertion mutations identified in the spike protein.

Table 1
Nucleotide and amino acid difference of human coronaviruses (HCoVs)-OC43 (759 → 1558).

Coding sequence	Nucleotide	Amino acid
1ab	C1158A	R317C
	C1240A	A344V
	G1487T	M426I
	T1924C	F572S
	C2647A	A813N
	C5259T	H1684Y
	C7652T	S2488F
	A8986G	N2926S
	A11555C	R3782S
	T16840A	S5545R
	A18384C	D6059A
	G18569A	G6121S
NS2	C21991T	P162P
	G22145T	V214L
HE	T23498C	L392S
	C23500T	P393S
S	23715insertCTAGTT	D24-I26insTSY
	C24805T	T148I
	A24190G	H183R
	T23463C	Y241H
	24420insertAGGATGGTTTTA	K259-T260insVKNGF
	A24735G	S365G
	G24805C	G388A
	25242insertAAGCTA	P533-T534insKAT
	G25903T	R754I
	T26047A	V802E
	C26247T	L869C
	T26248G	L869C
	26340insertTCAATGCTTATG	K899-A900insVNAYA
	T26562G	W974L
	C26563T	W974L
	G26577C	G979R
	G26972C	M1110I
	C26993T	V1117V
	T27280G	V1213G
	C27488T	I1282I
	A27542G	V1300V
N	T29157G	F33V

4. Discussion

The reverse genetic system represents one of the most powerful tools in molecular virology, enabling the genetic manipulation of infectious recombinant virus from a cDNA clone of the viral genome. However, the assembling of full-length cDNA clones for CoVs poses significant challenges due to their large viral genome size, the presence of bacteria-toxic features, cryptic transcription elements, splicing mechanisms, recombination events and termination signals, all of which can lead to deleterious mutations [39].

Our prior research found that inserting a reporter gene into the ns2 region rescues rOC43(759) successfully, whereas modifications to ns12.9 do not yield similar results [28,29]. In this study, we report for the first time, the successful application of a one-step assembly

Fig. 4. Biological characteristics of HCoVs-OC43-VR1558 and HCoV-OC43-VR759. A) Bright-field images of the BHK-21 cells infected with different viruses. Cytopathic effects (CPE) were observed at 144 h post-transfection. Representative images of mock-infected and transfected cells are shown. Scale bars: 200 μm. B) Time course analysis of the reporter gene expression. Cells were either mock-infected or infected (MOI of 0.01) with rOC43(1558)-ns2FusionRluc and rOC43 (759)-ns2DelRluc. At 48 h post-infection, Rluc expression in cell culture supernatants were analysed using the Renilla-Glo luciferase assay system. C) – G) Mice were infected with the rOC43(759)-ns2DelRluc, rOC43(1558)-ns2FusionRluc and rOC43(1558)-WT. Notably, 10-day-old suckling mice were either mock-(PBS) infected or infected with different doses of rOC43 (n = 4 / group). Body weight (C) and survival (D) were evaluated at the indicated days post-infection. Mice that lost 25 % of their initial body weight were humanely euthanized. Error bars represent the standard deviations of the mean for each group. E) BLI of BALB / c mice after infection with rOC43(1558)-ns2FusionRluc (10^6 $TCID_{50}$) and rOC43(759)-ns2DelRluc (10^2 $TCID_{50}$). BLI was performed daily by intraperitoneal injection of Rluc substrate and capture of photon emission using the *in vivo* F Pro system. Representative BLI images are shown. F) Histology of brain sections. Brains were sectioned for hematoxylin and eosin (H & E) staining. G) The presence of each virus load in various tissues of mice (brain, lung, liver, spleen, kidney, respectively). Abbreviations: HCoVs, human coronaviruses; MOI, multiplicity of infection; $TCID_{50}$, 50 % tissue culture infective dose; BLI, bioluminescence imaging; Rluc, Renilla luciferase; WT, wild type; RLU, relative light unit; PBS, phosphate buffered saline.

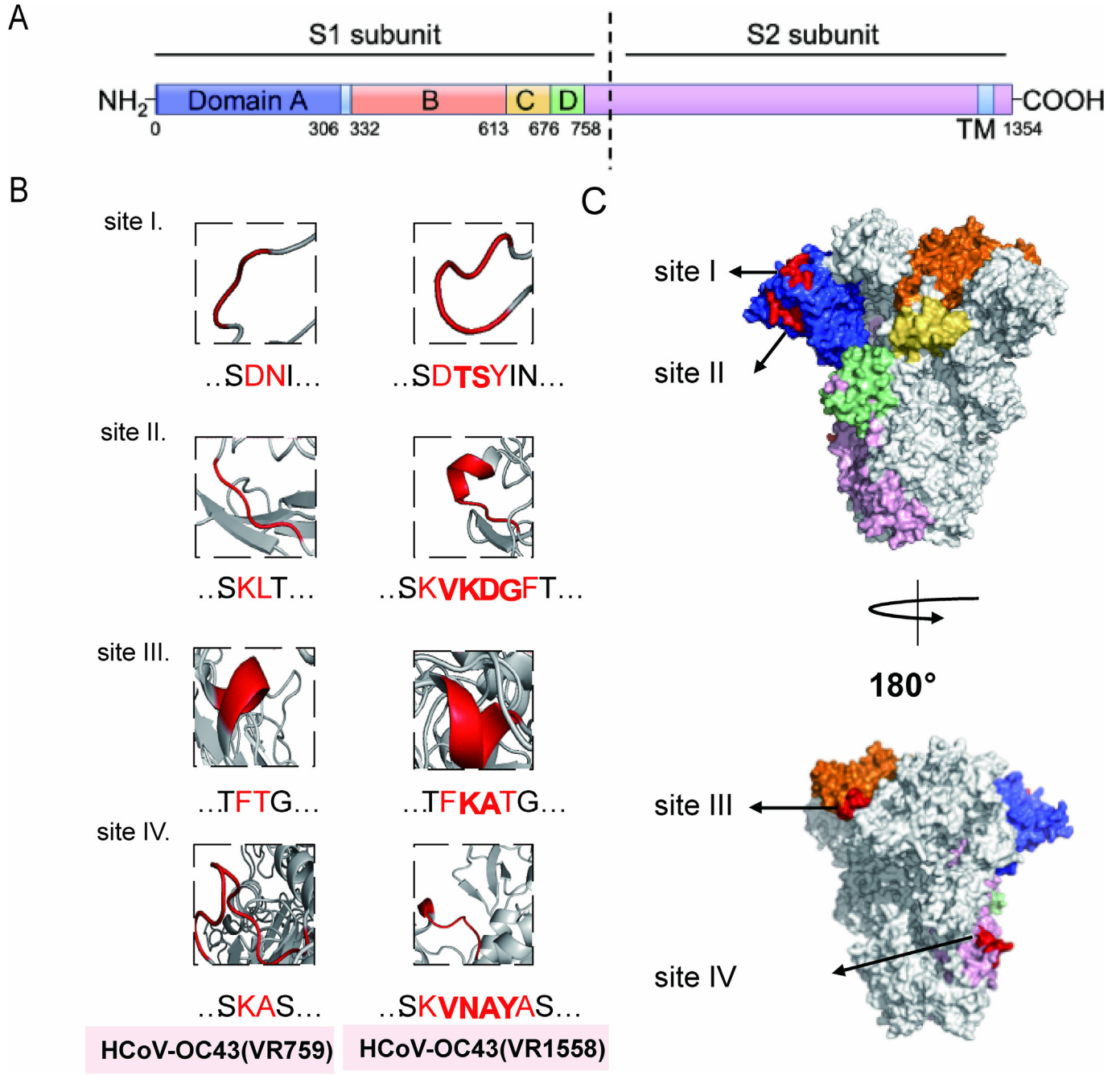

Fig. 5. Structure of the human coronaviruses (HCoVs)-OC43 spike glycoprotein predicted by SWISS-MODEL homology modelling. Models were generated using the spike structure of HCoV-OC43. A) Schematic diagram of the S glycoprotein organization. B) – C) Surface representation of the OC43 spike protein. The rectangle shows amino acid insertion sites.

technique in yeast for the rapid generation of recombinant HCoV-OC43-VR1558 wild type (WT) or with reporters. This approach provide a valuable platform for the investigation of viral biology and screening of inhibitors for HCoVs.

Although several ICs of the HCoV-OC43-VR759 have been developed and used for subsequent studies, the tissue culture-adapted HCoV-OC43-VR1558, derived from a virus passaged in mice (HCoV-OC43-VR759), has not been reported to possess the ability to develop an infectious clone. Our reverse genetics approach on HCoV-OC43 using TAR enabled us to rescue rOC43(1558)-WT and rOC43(1558)-stably expressing the Rluc reporter gene. We partially edited ns2 region and incorporated reporter genes, which showed no significant impact on viral replication. The feasibility of removing viral genes and inserting reporter genes demonstrates the genetic plasticity of the HCoV-OC43 genome and suggests the possibility of generating recombinant viruses. Reporter-expressing replicating competent viruses can be used to monitor viral infections, assess viral fitness, and evaluate and/or identify antivirals, and reporter gene expression can be used as a valid surrogate for virus detection in infected cells [12]. Notably, despite genome editing of ns2 and the insertion of a reporter gene, the reporter-expressing rHCoV-OC43 constructs exhibited growth kinetics similar to those of their wild-type counterparts.

This observation suggests that the ns2 region may not be a critical element for HCoV-OC43 replication. As expected, viral infection was observed in real-time, alleviating the need for additional approaches to detect the virus in infected cells. The correlation between the kinetics of the reporter gene and the level of viral replication underscores the efficacy of using these reporter genes as reliable surrogates to assess viral infection.

The antiviral properties of remdesivir and chloroquine have been previously reported. In this study, we demonstrated that reporter-expressing rHCoV-OC43 constructs provide a robust platform for the rapid identification and characterization of antivirals for the therapeutic and/or prophylactic treatment of HCoV-OC43 infections. Multiple factors contribute to this difference, including the sensitivity of the methods, the variations in cell states, and the potential errors inherent in experimental techniques. The EC_{50} determined by percent viral copies is a classic method that relied on the proliferation of viral nucleic acids, while the Rluc activity method is fundamentally based on the activity of luciferase and the interpretation of substrate results, influenced by factors such as substrate expression, cell stability, and enzyme activity. For remdesivir, the EC_{50} results are different by 3-fold for percent viral copies and percent RLuc activity, while a difference of about 23 % is observed for chloroquine. These differences may be related to the distinct anti-viral mechanisms between remdesivir and chloroquine, and the sensitive and influences factor for these methods. Nonetheless, the results remained within an acceptable range of effective concentrations. Importantly, the EC_{50} obtained for our reporter-expressing viruses were consistent with those reported in previously studies, demonstrating the feasibility of using our reporter-based assays for the rapid identification of antivirals [28,40,41].

Moreover, we further evaluated the feasibility of using rOC43 (1558)-ns2FusionRluc in mice. Infection of mice by HCoV-OC43 was affected by many variables, such as the virus strains, the route of inoculation, the challenge dose, mice age and its genetic background [35]. Previous studies showed that BALB/c mice were more resistant than C57BL / 6 when infected with the same dose HCoV-OC43, researchers have tried different inoculation routes to analysis the properties of HCoV-OC43 in BALB / c and C57BL / 6 mice, such as intraperitoneal, intraoral, and intranasal inoculation route, their results showed that the viral RNA was mainly found in the brain for the 1-week-old mice, but could not detect the virus in tissues of spinal cord, heart, lung, liver, and spleen, indicated the neurotropic and neuroinvasive properties of HCoV-OC43 in mice [27,35]. In this study, we focus on the different virulence of HCoV-OC43 VR759 and VR1558, so the intracerebral inoculation method of infection was chosen. This model provides a compelling visualization of neurological symptoms caused by coronavirus infection in real-time, allowing us to illustrate both geographical and temporal progression of the infection. Additionally, it facilitates the evaluation of broad-spectrum anti-coronavirus inhibitors *in vitro* and *in vivo*.

Furthermore, the differences between HCoV-OC43-VR759 and HCoV-OC43-VR1558 were compared both *in vitro* and *in vivo*. *In vitro*, BHK-21 cells infected with rOC43(1558)-WT and rOC43(1558)-ns2FusionRluc- exhibited significant cytopathic effects, whereas BHK-21 cells incubated with rOC43(759)-WT and rOC43(759)-ns2DelRluc showed no cytopathic effects. Several investigations were conducted with the VR759 strains in our previous work [27,28]. With a specific focused on the capabilities of the reporter system of VR1558 strains, allowing for quantitative measurement and real time monitor of virulent, we used the recombinant rOC43(759)-ns2DelRluc as a positive control and compare the virulence for rOC43(1558)-ns2FusionRluc to that of rOc43(1558)-WT. Based on assessments of changes in mice body weight, survival rate and neurological symptoms, our results demonstrated that the virulence for rOC43(1558)-ns2FusionRluc is comparable to that of rOc43(1558)-WT, but less virulent when compared to that of rOC43(759)-ns2DelRluc, the real-time luciferase signals were consistent to that of the clinical symptoms.

According to the references, HCoV-OC43 was originally isolated after passage in human embryonic tracheal organ cultures, this virus caused neurological disease in suckling mice (termed HCoV-$OC43_{NV}$) [42]. Subsequently, this virus was propagated in tissue culture cells and generating a tissue culture-adapted variant (termed HCoV-$OC43_{TC}$). In fact, most recent studies have used neurovirulent viruses that have undergone further propagated in tissue culture cells [35]. HCoV-OC43 is known to possesses inherent neuroinvasive and neurotropic properties in humans [43]. Nevertheless, the direct link between HCoV-OC43 and neurological disorders remains unsubstantiated [44]. Studies have identified mutations in the spike glycoprotein due to the continuous proliferation of HCoV-OC43 in human brain cell cultures. Infection with HCoV-OC43 containing two amino acids mutations in the spike glycoprotein (rOC / Us183-241) led to a significant increase in cell death in both murine and human neural cells [45]. Specifically, the point mutations in the S glycoproteins (H183R and Y241H), the mutant HCoV-OC43 caused a more pronounced unfolded protein response and reduced protein translation. Therefore, this mutant virus led to greater neuronal damage and was associated with increased viral spread, enhanced T-c-cell infiltration, and elevated release of cytokines that promote inflammation [46,47]. These findings may explain why the CPE of HCoV-OC43-VR1558 was more significant in BHK-21 cell lines compared with HCoV-OC43-VR759. As mutants of H183R and Y241H in S protein resulted in a significant increase in cell death in both murine and human neuro cells, caused an increased neuronal cell death by apoptosis.

Effective cleavage of the spike protein is associated with the neurovirulence of HCoV-OC43 [48]. A previous study demonstrated that the modified sequence KASSAS (derived from the original KASSRS) renders the HCoV-OC43 virus becoming avirulent, as indicated by the absence of neurological symptoms and mortality [48]. Notably, in the present study, five amino acids were inserted at the putative S2′ position (K899 A900insVNAYA). Data from animal experiment indicated a significant reduction in neurovirulence compared to HCoV-OC43-VR759, likely attributable to the inhibition of protease cleavage.

While the luciferase reporter system provides advantages for studying viral replication and evaluating antiviral agents, it also presents notable limitations. The requirement for luciferin substrate and specialized chemiluminescence instrumentation pose practical challenges. However, this limitation could potentially be overcome by replacing the luciferase reporter in rOC43(1558)-ns2FusionRluc with alternative reporter.

In summary, we successfully generated a robust and stable luciferase-based recombinant HCoV-OC43 strain by replacing ns2 and employing the TAR strategy. To the best of our knowledge, this is the first report detailing the construction of a HCoV-OC43-VR1558 IC and a systematic comparison with the prototype strain, HCoV-OC43-VR759. This reporter virus is expected to apply on screening for broad-spectrum drugs or host factors that influence HCoV replication. The rapid construction and comprehensive application of an IC system for coronavirus facilitates further research on virus biology and its mechanisms, improved diagnostic tests, vaccine production, and screening antiviral compounds.

Ethics statement

This study was reviewed and approved by the Ethics Committee of the Chinese Center for Disease Control and Prevention (approval number 20220309034).

Acknowledgements

This work was supported by the National Key Research and Development Program of China (2022YFC2304100 and 2021YFA1201003).

Conflcit of interest statement

The authors declare that there are no conflicts of interest.

Author contributions

Fei Ye: Writing – original draft, Data curation. **Na Wang:** Writing – original draft, Data curation. **Qiongge Guan:** Writing – original draft, Methodology, Data curation. **Mengwei Wang:** Writing – original draft, Methodology, Data curation. **Jiewei Sun:** Writing – original draft, Data curation. **Desheng Zhai:** Writing – review & editing, Methodology. **Baoying Huang:** Writing – review & editing, Methodology, Funding acquisition, Conceptualization. **Ying Zhao:** Writing – review & editing, Methodology, Conceptualization. **Wenjie Tan:** Writing – review & editing, Resources, Methodology, Funding acquisition, Conceptualization.

Supplementary data

Supplementary data to this article can be found online at https://doi.org/10.1016/j.bsheal.2024.11.006.

References

[1] C. Huang, Y. Wang, X. Li, L. Ren, J. Zhao, Y. Hu, L. Zhang, G. Fan, J. Xu, X. Gu, et al., Clinical features of patients infected with 2019 novel coronavirus in Wuhan, China, Lancet 395 (2020) 497–506, https://doi.org/10.1016/S0140-6736(20)30183-30185.

[2] N. Zhu, D. Zhang, W. Wang, X. Li, B. Yang, J. Song, X. Zhao, B. Huang, W. Shi, R. Lu, et al., A novel coronavirus from patients with pneumonia in China, 2019, N. Engl. J. Med. 382 (2020) 727–733, https://doi.org/10.1056/NEJMoa2001017.

[3] H. Cai, Y. Huang, Reverse genetics systems for SARS-CoV-2: Development and applications, Virol. Sin. 38 (2023) 837–850, https://doi.org/10.1016/j.virs.2023.10.001.

[4] S.H. van den Worm, K.K. Eriksson, J.C. Zevenhoven, F. Weber, R. Züst, T. Kuri, R. Dijkman, G. Chang, S.G. Siddell, E.J. Snijder, Davidson, et al., Reverse genetics of SARS-related coronavirus using vaccinia virus-based recombination, PLoS One 7 (2012) e32857, https://doi.org/10.1371/journal.pone.0032857.

[5] X. Xie, A.E. Muruato, X. Zhang, K.G. Lokugamage, C.R. Fontes-Garfias, J. Zou, J. Liu, P. Ren, M. Balakrishnan, T. Cihlar, et al., A nanoluciferase SARS-CoV-2 for rapid neutralization testing and screening of anti-infective drugs for COVID-19, Nat. Commun. 11 (2020) 5214, https://doi.org/10.1038/s41467-020-19055-7.

[6] J.M. Gonzalez, Z. Penzes, F. Almazan, E. Calvo, L. Enjuanes, Stabilization of a full-length infectious cDNA clone of transmissible gastroenteritis coronavirus by insertion of an intron, J. Virol. 76 (2002) 4655–4661, https://doi.org/10.1128/jvi.76.9.4655-4661.2002.

[7] P.S. Masters, Reverse genetics of the largest RNA viruses, Adv. Virus Res. 53 (1999) 245–265, https://doi.org/10.1016/s0065-3527(08)60351-6.

[8] A.H. Malczyk, A. Kupke, S. Prüfer, V.A. Scheuplein, S. Hutzler, D. Kreuz, T. Beissert, S. Bauer, S. Hubich-Rau, C. Tondera, et al., A Highly immunogenic and protective Middle East Respiratory Syndrome Coronavirus vaccine based on a recombinant measles virus vaccine platform, J. Virol. 89 (2015) 11654–11667, https://doi.org/10.1128/JVI.01815-15.

[9] V. Thiel, J. Herold, B. Schelle, S.G. Siddell, Infectious RNA transcribed *in vitro* from a cDNA copy of the human coronavirus genome cloned in vaccinia virus, J. Gen. Virol. 82 (2001) 1273–1281, https://doi.org/10.1099/0022-1317-82-6-1273.

[10] E.F. Donaldson, B. Yount, A.C. Sims, S. Burkett, R.J. Pickles, R.S. Baric, Systematic assembly of a full-length infectious clone of human coronavirus NL63, J. Virol. 82 (2008) 11948–11957, https://doi.org/10.1128/JVI.01804-08.

[11] Y.J. Hou, K. Okuda, C.E. Edwards, D.R. Martinez, T. Asakura, K.H. Dinnon, T. Kato, R.E. Lee, B.L. Yount, T.M. Mascenik, et al., SARS-CoV-2 reverse genetics reveals a variable infection gradient in the respiratory tract, Cell 182 (2020) 429–446. e414, https://doi.org/10.1016/j.cell.2020.05.042.

[12] K. Chiem, D. Morales Vasquez, J.G. Park, R.N. Platt, T. Anderson, M.R. Walter, J.J. Kobie, C. Ye, L. Martinez-Sobrido, Generation and characterization of recombinant SARS-CoV-2 expressing reporter genes, J. Virol. 95 (2021) e02209–e02220, https://doi.org/10.1128/JVI.02209-20.

[13] J.R. St-Jean, M. Desforges, F. Almazan, H. Jacomy, L. Enjuanes, P.J. Talbot, Recovery of a neurovirulent human coronavirus OC43 from an infectious cDNA clone, J. Virol. 80 (2006) 3670–3674, https://doi.org/10.1128/JVI.80.7.3670-3674.2006.

[14] A.M. Nikiforuk, A. Leung, B.W.M. Cook, D.A. Court, D. Kobasa, S.S. Theriault, Rapid one-step construction of a Middle East Respiratory Syndrome (MERS-CoV) infectious clone system by homologous recombination, J. Virol. Methods 236 (2016) 178–183, https://doi.org/10.1016/j.jviromet.2016.07.022.

[15] T. Thi Nhu Thao, F. Labroussaa, N. Ebert, P. V'Kovski, H. Stalder, J. Portmann, J. Kelly, S. Steiner, M. Holwerda, A. Kratzel, M. Gultom, K. Schmied, et al., Rapid reconstruction of SARS-CoV-2 using a synthetic genomics platform, Nature 582 (2020) 561–565, https://doi.org/10.1038/s41586-020-2294-9.

[16] B. Wang, C. Zhang, X. Lei, L. Ren, Z. Zhao, J. Wang, H. Huang, Construction of non-infectious SARS-CoV-2 replicons and their application in drug evaluation, Virol. Sin. 36 (2021) 890–900, https://doi.org/10.1007/s12250-021-00369-9.

[17] A.A. Amarilla, J.D.J. Sng, R. Parry, J.M. Deerain, J.R. Potter, Y.X. Setoh, D.J. Rawle, T.T. Le, N. Modhiran, X. Wang, et al., A versatile reverse genetics platform for SARS-CoV-2 and other positive-strand RNA viruses, Nat. Commun. 12 (2021) 3431, https://doi.org/10.1038/s41467-021-23779-5.

[18] S. Torii, C. Ono, R. Suzuki, Y. Morioka, I. Anzai, Y. Fauzyah, Y. Maeda, W. Kamitani, T. Fukuhara, Y. Matsuura, Establishment of a reverse genetics system for SARS-CoV-2 using circular polymerase extension reaction, Cell Rep. 35 (2021) 109014, https://doi.org/10.1016/j.celrep.2021.109014.

[19] J. Melade, G. Piorkowski, F. Touret, T. Fourie, J.S. Driouich, M. Cochin, H.S. Bouzidi, B. Coutard, A. Nougairede, X. de Lamballerie, A simple reverse genetics method to generate recombinant coronaviruses, EMBO Rep. 23 (2022) e53820, https://doi.org/10.15252/embr.202153820.

[20] L. Mao, H. Jin, M. Wang, Y. Hu, S. Chen, Q. He, J. Chang, C. Hong, Y. Zhou, D. Wang, et al., Neurologic manifestations of hospitalized patients with coronavirus disease 2019 in Wuhan, China, JAMA Neurology 77 (2020) 683–690, https://doi.org/10.1001/jamaneurol.2020.1127.

[21] M. Saad, A.S. Omrani, K. Baig, A. Bahloul, F. Elzein, M.A. Matin, M.A.A. Selim, M. A. Mutairi, D.A. Nakhli, A.Y.A. Aidaroos, et al., Clinical aspects and outcomes of 70 patients with Middle East respiratory syndrome coronavirus infection: a single-center experience in Saudi Arabia, Int. J. Infect. Dis. 29 (2014) 301–306, https://doi.org/10.1016/j.ijid.2014.09.003.

[22] S. Morfopoulou, J.R. Brown, E.G. Davies, G. Anderson, A. Virasami, W. Qasim, W. K. Chong, M. Hubank, V. Plagnol, M. Desforges, et al., Human coronavirus OC43 associated with fatal encephalitis, N. Engl. J. Med. 375 (2016) 497–498, https://doi.org/10.1056/NEJMc1509458.

[23] Y. Gerchman, H. Mamane, N. Friedman, M. Mandelboim, UV-LED disinfection of coronavirus: Wavelength effect, J. Photochem. Photobiol. 212 (2020) 112044, https://doi.org/10.1016/j.jphotobiol.2020.112044.

[24] E. Brison, H. Jacomy, M. Desforges, P.J. Talbot, Glutamate excitotoxicity is involved in the induction of paralysis in mice after infection by a human coronavirus with a single point mutation in its spike protein, J. Virol. 85 (2011) 12464–12473, https://doi.org/10.1128/JVI.05576-11.

[25] M. Desforges, J. Desjardins, C. Zhang, P.J. Talbot, The acetyl-esterase activity of the hemagglutinin-esterase protein of human coronavirus OC43 strongly enhances the production of infectious virus, J. Virol. 87 (2013) 3097–3107, https://doi.org/10.1128/JVI.02699-12.

[26] A.L. Coupanec, M. Desforges, B. Kaufer, P. Dubeau, M. Cote, P.J. Talbot, Potential differences in cleavage of the S protein and type-1 interferon together control human coronavirus infection, propagation, and neuropathology within the central nervous system, J. Virol. 95 (2021) e00140–e00221, https://doi.org/10.1128/JVI.00140-21.

[27] J. Niu, L. Shen, B. Huang, F. Ye, L. Zhao, H. Wang, Y. Deng, W. Tan, Non-invasive bioluminescence imaging of HCoV-OC43 infection and therapy in the central nervous system of live mice, Antiviral Res. 173 (2019) 104646, https://doi.org/10.1016/j.antiviral.2019.104646.

[28] L. Shen, J. Niu, C. Wang, B. Huang, W. Wang, N. Zhu, Y. Deng, H. Wang, F. Ye, S. Cen, et al., High-throughput screening and identification of potent broad-spectrum inhibitors of coronaviruses, J. Virol. 93 (2019) e00023–e00119, https://doi.org/10.1128/JVI.00023-19.

[29] L. Shen, Y. Yang, F. Ye, G. Liu, M. Desforges, P.J. Talbot, W. Tan, Safe and sensitive antiviral screening platform based on recombinant human coronavirus OC43 expressing the luciferase reporter gene, Antimicrob. Agents Chemother. 60 (2016) 5492–5503, https://doi.org/10.1128/AAC.00814-16.

[30] J.K. Stodola, G. Dubois, A.L. Coupanec, M. Desforges, P.J. Talbot, The OC43 human coronavirus envelope protein is critical for infectious virus production and propagation in neuronal cells and is a determinant of neurovirulence and CNS pathology, Virology 515 (2018) 134–149, https://doi.org/10.1016/j.virol.2017.12.023.

[31] R. Zhang, K. Wang, X. Ping, W. Yu, Z. Qian, S. Xiong, B. Sun, S. Perlman, The ns12.9 accessory protein of human coronavirus OC43 is a viroporin involved in virion morphogenesis and pathogenesis, J. Virol. 89 (2015) 11383–11395, https://doi.org/10.1128/JVI.01986-15.

[32] M.V. Diefenbacher, T.J. Baric, D.R. Martinez, R.S. Baric, N.J. Catanzaro, T.P. Sheahan, A nano-luciferase expressing human coronavirus OC43 for countermeasure development, Virus Res. 339 (2024) 199286, https://doi.org/10.1016/j.virusres.2023.199286.

[33] N. Kouprina, V. Larionov, Selective isolation of genomic loci from complex genomes by transformation-associated recombination cloning in the yeast *Saccharomyces cerevisiae*, Nat. Protoc. 3 (2008) 371–377, https://doi.org/10.1038/nprot.2008.5.

[34] Y. Zhou, C. Li, C. Ren, J. Hu, C. Song, X. Wang, Y. Li. One-step assembly of a Porcine Epidemic Diarrhea Virus infectious cDNA clone by homologous recombination in Yeast: Rapid manipulation of viral genome with CRISPR/Cas9 gene-editing technology, Front. Microbiol. 13 (2022) 787739, https://doi.org/10.3389/fmicb.2022.787739.

[35] H. Jacomy, P.J. Talbot, Vacuolating encephalitis in mice infected by human coronavirus OC43, Virology 315 (2023) 20–33, https://doi.org/10.1016/S0042-6822(03)00323-4.

[36] N. Butler, L. Pewe, K. Trandem, S. Perlman, Murine encephalitis caused by HCoV-OC43, A human coronavirus with broad species specificity, is partly immune-

mediated, Virology 347 (2006) 410–421, https://doi.org/10.1016/j.virol.2005.11.044.
[37] J.R. St-Jean, H. Jacomy, M. Desforges, A. Vabret, F. Freymuth, P.J. Talbot, Human respiratory coronavirus OC43: Genetic stability and neuroinvasion, J Virol. 78 (2004) 8824–8834, https://doi.org/10.1128/JVI.78.16.8824-8834.2004.
[38] L. Vijgen, E. Keyaerts, E. Moës, I. Thoelen, E. Wollants, P. Lemey, A.M. Vandamme, M. Van Ranst, Complete genomic sequence of human coronavirus OC43: Molecular clock analysis suggests a relatively recent zoonotic coronavirus transmission event, J. Virol. 79 (2005) 1595–1604, https://doi.org/10.1128/JVI.79.3.1595-1604.2005.
[39] F. Almazan, I. Sola, S. Zuniga, S. Marquez-Jurado, L. Morales, M. Becares, L. Enjuanes, Coronavirus reverse genetic systems: infectious clones and replicons, Virus Res. 189 (2014) 262–270, https://doi.org/10.1016/j.virusres.2014.05.026.
[40] A.J. Brown, J.J. Won, R.L. Graham, K.H. Dinnon, A.C. Sims, J.Y. Feng, T. Cihlar, M. R. Denison, R.S. Baric, T.P. Sheahan, Broad spectrum antiviral remdesivir inhibits human endemic and zoonotic deltacoronaviruses with a highly divergent RNA dependent RNA polymerase, Antiviral Res. 169 (2019) 104541, https://doi.org/10.1016/j.antiviral.2019.104541.
[41] L. Persoons, E. Vanderlinden, L. Vangeel, X. Wang, N.D.T. Do, S.Y.C. Foo, P. Leyssen, J. Neyts, D. Jochmans, DSchols, et al., Broad spectrum anti-coronavirus activity of a series of anti-malaria quinoline analogues, Antiviral Res. 193 (2021) 105127, https://doi.org/10.1016/j.antiviral.2021.105127.
[42] K. McIntosh, W.B. Becker, R.M.Chanock, Growth in suckling-mouse brain of "IBV-like" viruses from patients with upper respiratory tract disease, Proc. Natl. Acad. Sci. U.S.A. 58 (1967) 2268–2273, https://doi.org/10.1073/pnas.58.6.2268.
[43] Y. Wu, X. Xu, Z. Chen, J. Duan, K. Hashimoto, L. Yang, C. Liu, C. Yang, Nervous system involvement after infection with COVID-19 and other coronaviruses, Brain Behav. Immun. 87 (2020) 18–22, https://doi.org/10.1016/j.bbi.2020.03.031.
[44] M. Desforges, A.L. Coupanec, P. Dubeau, A. Bourgouin, L. Lajoie, M. Dube, P.J. Talbot, Human coronaviruses and other respiratory viruses: underestimated opportunistic pathogens of the central nervous system, Viruses 12 (2019) 14, https://doi.org/10.3390/v12010014.
[45] M. Meessen-Pinard, A.L. Coupanec, M. Desforges, P.J. Talbot, D.S. Lyles, Pivotal role of receptor-interacting protein kinase 1 and mixed lineage kinase domain-like in neuronal cell death induced by the human neuroinvasive coronavirus OC43, J. Virol. 91 (2016) e01513–16, https://doi.org/10.1128/JVI.01513-16.
[46] D.J. Favreau, M. Desforges, J.R. St-Jean, P.J. Talbot, A human coronavirus OC43 variant harboring persistence-associated mutations in the S glycoprotein differentially induces the unfolded protein response in human neurons as compared to wild-type virus, Virology 395 (2009) 255–267, https://doi.org/10.1016/j.virol.2009.09.026.
[47] H. Jacomy, J.R. St-Jean, E. Brison, G. Marceau, M. Desforges, P.J. Talbot, Mutations in the spike glycoprotein of human coronavirus OC43 modulate disease in BALB/c mice from encephalitis to flaccid paralysis and demyelination, J Neurovirol. 16 (2010) 279–293, https://doi.org/10.3109/13550284.2010.497806.
[48] A.L. Coupanec, M. Desforges, M.P. Meessen, M. Dube, R. Day, N.G. Seidah, P.J. Talbot, Cleavage of a neuroinvasive human respiratory virus spike glycoprotein by proprotein convertases modulates neurovirulence and virus spread within the central nervous system, PLoS Pathog. 11 (2015) e1005261, https://doi.org/10.1371/journal.ppat.1005261.